Your Hohm
Tri-Directional and Localized Coherence: The Geometry of Observation and Perception
Part II of the U.R.H.U.E.0hm Series
ZPIP — The Zero Point of Infinite Potentiality
0hm

Talon

hohm.cc

November 22, 2025

Abstract

This work extends the U.R.H.U.E.0hm (Unfolding Resonant Harmonic Unity Emergence) framework developed in Part I, where the triadic generative structure and the 3–9–27 cascade were introduced as a candidate underlying pattern for physical constants and scaling relations.

Here, the focus shifts from numerical structure to a geometrical and dynamical picture of *coherence* and *observation*. Reality is modeled as a single underlying process that continuously folds back into itself, leaving graded traces and generating localized regions of high self-intersection. These regions appear as matter, fields, and experiential nodes.

An observer-centered geometry is introduced using circular cross-sections in which straight-through trajectories, changing only in angle, produce wave-like appearances. A coherence field measures self-overlap of the process with its own history. Localized curvature in this coherence field acts as a lens for trajectories, offering a way to describe redshift-like effects and apparent large-scale recession without assuming an overall global expansion.

The goal is not to present a final closed formalism, but to offer a coherent geometric and mathematical scaffolding that ties the 3–9–27 structure, tri-directional flow, and observer-centric perception into one narrative that can be refined, tested, and extended.

Contents

1 Relation to Part I and the 3–9–27 Cascade

In Part I of the U.R.H.U.E.0hm series, the starting point was a numerical and structural axiom: reality emerges from a triadic generative scheme whose simplest manifestation is the 3–9–27 cascade and its higher-order extensions.

A representative block (schematically) of the kind of structure considered there is:

$$\begin{aligned}[1][1]\{3,9,27 \ \langle\rangle\ 81,243,729 \ \diamond\ 2{,}187,6{,}561,19{,}683 \\ \langle\rangle\ 59{,}049,177{,}147,531{,}441 \ \diamond\ 1{,}594{,}323\}^{13}\{\cdots\}\end{aligned} \tag{1}$$

with further layers and mirrored structures (e.g. $1 \leftrightarrow 13$) encoding a specific cascade and breathing pattern. Here the notation $[k][\ell]\{\cdots\}$, angle brackets, and diamonds are placeholders for the detailed pattern introduced in Part I.

The present work assumes this generative structure as the seed and focuses on:

- how a tri-directional, numerically constrained process can be represented in observer-centered geometry;
- how self-intersection and graded memory can be captured by a coherence field;
- how localized curvature in that field may affect observation and perceived redshifts.

2 Single Underlying Process and Coherence

2.1 One process, tri-directional structure

We take as axiom:

> There is one underlying process. Apparent multiplicity of lines, waves, objects, or observers arises from viewing different phases and angles of this one process as if they were separate.

We represent the process abstractly by a field

$$\phi(\mathbf{x}, t), \tag{2}$$

where $(\mathbf{x}, t)$ is a spacetime-like coordinate. Tri-directionality is reflected in the idea that at each $(\mathbf{x}, t)$, the process has three coupled "modes":

$$\phi(\mathbf{x}, t) \sim \big(\phi_1(\mathbf{x}, t),\ \phi_2(\mathbf{x}, t),\ \phi_3(\mathbf{x}, t)\big), \tag{3}$$

related by internal constraints rather than being fully independent fields.

2.2 Graded memory and self-overlap

As the process unfolds, it leaves a graded trail or memory in its own configuration space. A simple way to encode this is via a self-overlap functional:

$$I(\mathbf{x}, t) = \int_{-\infty}^{t} G(t - t')\, \mathcal{F}\big(\phi(\mathbf{x}, t), \phi(\mathbf{x}, t')\big)\, dt', \tag{4}$$

where

- $G(\tau)$ is a memory kernel (e.g. $G(\tau) = e^{-\tau/\tau_0}$ for $\tau \geq 0$),
- $\mathcal{F}$ measures similarity or intersection between the current state and its past state at the same location.

From $I(\mathbf{x}, t)$ we define a *coherence field*:

$$\kappa(\mathbf{x}, t) = H\big(I(\mathbf{x}, t)\big), \tag{5}$$

where H is monotone, mapping overlap intensity into a measure of "how coherently this point is re-visiting itself."

2.3 Regimes of coherence

Different regimes of κ can be associated with different kinds of phenomena:

- very low κ: highly decoherent, transient fluctuations;
- intermediate κ: radiation-like, transmissive patterns;
- high κ: matter-like loci where self-intersection is strong and persistent;
- very high or specifically structured κ: nodes capable of sustaining complex, self-referential patterns (experience-like loci).

Thresholds such as κ_{light}, κ_{matter}, and κ_{exp} can be viewed as emergent scales, potentially related to the discrete ratios appearing in the 3–9–27 cascades.

3 Observer-Centered Circle Geometry

3.1 Setup: observer at the center

We now build a minimal geometric model in 2D that makes the observer structure explicit.

Let the observer be at the origin $\mathbf{x}_{\text{obs}} = (0, 0)$. Consider the unit circle:

$$x^2 + y^2 = 1. \tag{6}$$

This circle is a cross-section through a larger configuration space (generalizable to a sphere in 3D).

The underlying process, at a given phase, appears as a straight line through the center at angle θ:

$$L_\theta(s) = (s\cos\theta,\ s\sin\theta), \quad s \in \mathbb{R}. \tag{7}$$

These L_θ are not distinct entities, but different angular states of the one process.

3.2 Diagram: circle and straight-through trajectories

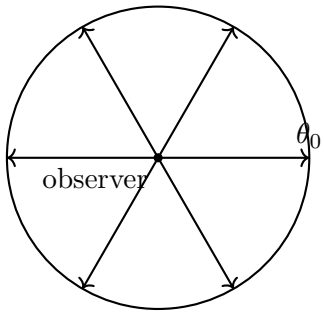

Figure 1: Observer-centered circle model. Straight lines through the center at angles separated by 120° represent tri-directional phases of a single underlying process.

Figure 1 shows the observer at the center and three privileged directions separated by 120°, corresponding to one possible representation of tri-directionality.

3.3 Angle modulation and wave-like appearance

Let the process be represented, from the observer's perspective, by a line at angle $\theta(t)$:

$$\theta(t) = \omega t + \theta_0 \tag{8}$$

for some angular frequency ω.

If the observer has a preferred direction (say the x-axis), one can define a simple intensity:

$$I_{\text{obs}}(t) = f\big(\cos(\theta(t))\big), \tag{9}$$

where f is maximal when $\cos(\theta)$ is near ± 1 and minimal when it is near 0.

This $I_{\text{obs}}(t)$ oscillates as $\theta(t)$ rotates, creating a wave-like pattern in time even though the underlying path $L_\theta(s)$ is always straight-through.

3.4 Two directions, one line

The same line can be viewed as having two opposed orientations:

$$L_{\theta+\pi}(s) = L_\theta(-s), \tag{10}$$

so at the center the "two directions" are indistinguishable. In the language of the model, these can be seen as counter-flowing phases of the same process, converging at the observational node.

3.5 Directional coherence

To connect the geometry to the coherence field, define a directional coherence relative to the observer:

$$\kappa_{\text{dir}}(\hat{\mathbf{n}}, t) = \int_0^\infty W(s)\, \kappa(\mathbf{x}_{\text{obs}} + s\,\hat{\mathbf{n}}, t)\, ds, \tag{11}$$

where $\hat{\mathbf{n}}$ is a unit vector and $W(s)$ is a decaying weight.

The direction that appears "flattest" or most natural is then:

$$\hat{\mathbf{n}}_{\text{flat}}(t) = \arg\max_{\hat{\mathbf{n}}}\, \kappa_{\text{dir}}(\hat{\mathbf{n}}, t). \tag{12}$$

In this sense, straightness is an emergent perception tied to coherence alignment, not an independent property of the underlying process.

4 Self-Intersection, Matter-Like Nodes, and Graded Trails

4.1 Graded curve model

Beyond the straight-line model, one can represent the process as a curve that loops back into its own graded trail. As a simple toy example in 2D:

$$\gamma(\tau) = \big(R(\tau)\cos(\omega\tau),\, R(\tau)\sin(\omega\tau)\big), \tag{13}$$

with a slowly varying radius $R(\tau)$ that "breathes":

$$R(\tau) = R_0 + \epsilon\sin(\Omega\tau), \tag{14}$$

where ϵ is small compared to R_0.

As τ evolves, $\gamma(\tau)$ traces out a spiral-like path that may intersect its own previous positions.

4.2 Self-intersection and coherence hotspot

We can define a simple local self-intersection density:

$$\rho_{\text{self}}(\mathbf{x}, t) = \int d\tau\, d\tau'\, K(t; \tau, \tau')\, \delta^{(2)}\big(\gamma(\tau) - \mathbf{x}\big)\, \delta^{(2)}\big(\gamma(\tau') - \mathbf{x}\big), \tag{15}$$

with K some kernel emphasizing near-simultaneous or specially correlated intersections.

Regions where ρ_{self} is high are candidates for matter-like or node-like structures.

Figure 2 is not a literal trajectory, but a qualitative picture of how repeated self-intersection in a small region can give rise to something that appears localized and persistent to an observer.

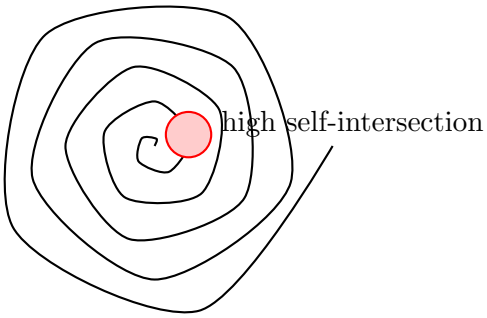

Figure 2: Schematic self-intersecting curve. A region where the curve repeatedly crosses itself can be treated as a coherence hotspot, analogous to a matter-like node.

5 Lensing from Coherence Gradients

5.1 Effective refractive index from coherence

We now let the coherence field $\kappa(\mathbf{x}, t)$ influence effective propagation. One toy model is:

$$n(\mathbf{x}, t) = n_0 + \alpha\, f\big(\kappa(\mathbf{x}, t)\big), \tag{16}$$

with f a function chosen so that regions of different κ correspond to different effective "speeds" or phase delays.

Light-like trajectories (or more generally, information-carrying patterns) then extremize an optical path:

$$S[\gamma] = \int_\gamma n(\mathbf{x}, t)\, ds, \tag{17}$$

where γ is a path and ds is a line element along it.

5.2 Diagram: coherence lens

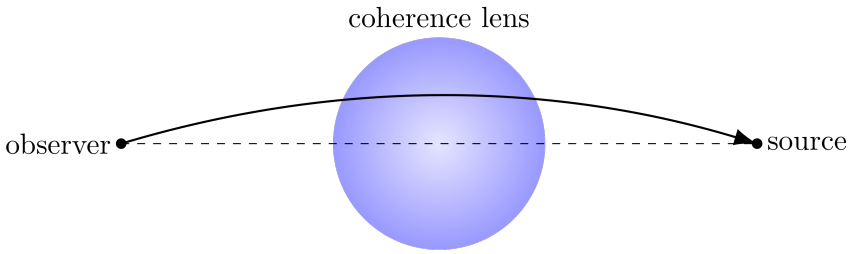

Figure 3: A region of altered coherence acting as a lens. A pattern that would travel straight in a uniform medium can be curved by a coherence gradient between source and observer.

Figure 3 illustrates how a localized coherence structure between source and observer can bend trajectories, similar to lensing, without invoking a global curvature at infinity.

5.3 Toy redshift model from path-dependent coherence

If a signal of intrinsic frequency ν_{emit} traverses a medium with spatially varying $n(\mathbf{x})$ and/or coupling to $\kappa(\mathbf{x})$, its observed frequency at the observer can be modeled as:

$$\nu_{\text{obs}} = \nu_{\text{emit}} \exp\Big(- \int_{\gamma} \beta(\mathbf{x})\, ds \Big), \tag{18}$$

where $\beta(\mathbf{x})$ is an effective stretching factor that depends on coherence properties along the path γ.

In such a model:

- Different paths from the same source to different observers can yield different redshifts.
- Even for a single observer, different directions in the sky could display different net redshift patterns depending on the coherence geometry around and between them.
- Regions organized in certain lattice-like or crystal-like patterns of $\kappa(\mathbf{x})$ could produce characteristic large-scale redshift distributions that are more about projection geometry than about uniform recession.

This is a *path-dependent* view of redshift, where the overall structure of the coherence field matters as much or more than a single global scale factor.

6 Perception, Flatness, and Curvature

6.1 Flatness as maximal coherence alignment

In the observer-centered picture, a direction is perceived as "flat" or "straight" when it aligns with a direction of high directional coherence $\kappa_{\text{dir}}(\hat{\mathbf{n}}, t)$ defined in Eq. (11).

This suggests:

> What we call a straight line is the direction in which the patterns arriving at us are most coherent and least obviously scrambled by cross-intersections.

Such "flat" directions may vary depending on the observer's position in the coherence landscape, and what appears flat at one scale may reveal complex curvature at another.

6.2 Curvature as layered coherence structure

Rather than thinking of curvature as a single geometric scalar describing all of space, this framework treats curvature as a layered manifestation of how the coherence field is structured across scales. Different layers (local, intermediate, very large-scale) can each exhibit their own patterns, and what appears as expansion, contraction, or steady-state behavior depends on how the observer samples those layers.

7 Cymatics, Pattern Formation, and Analogy

7.1 Cymatics as macroscopic analogy

Cymatic patterns—the organized shapes that emerge when a substrate is driven at certain frequencies—provide a macroscopic analogy to the behavior of the coherence field:

- Certain drive parameters produce highly symmetric, coherent patterns (analogous to high-κ configurations).
- Slight changes in parameters produce new patterns, sometimes via abrupt transitions.
- Nodes and anti-nodes of vibration determine where material accumulates or clears out, in direct analogy to coherent and decoherent regions.

In the U.R.H.U.E.0hm view, the underlying process is continuously driven, and the coherence thresholds act like implicit pattern selectors.

7.2 From analogy to modeling

While cymatics is not the same system as the fundamental process described here, a similar logic can be used:

1. Identify the base oscillatory structure (Part I: 3–9–27 and tri-directional flow).
2. Introduce thresholds where patterning shifts qualitatively (coherence thresholds).
3. Study how small changes in driving conditions or boundary conditions in κ produce large-scale structural changes.

This suggests numerical simulation as a next step: treat κ as a dynamical field and explore how different rules for ϕ and G in Eq. (4) generate structures that resemble matter, fields, and observer-loci.

8 Outlook and Further Directions

This Part II has aimed to:

- translate the U.R.H.U.E.0hm axiom and 3–9–27 structure into an explicit observer-centered geometry;
- formalize a coherence field as a measure of graded self-overlap of a single underlying process;
- show how tri-directional lines through a center circle can model wave-like appearance as angle modulation;
- sketch how coherence gradients can act as lenses and produce path-dependent redshift patterns.

Possible extensions include:

1. Mapping specific constants and scales in Part I directly to coherence thresholds and angular relations in the circle/sphere model.
2. Developing more concrete redshift predictions based on specific ansätze for $n(\mathbf{x}, t)$ and $\beta(\mathbf{x})$ in Eq. (18).
3. Writing a more openly philosophical and artistic Part III that discusses the implications of this picture for questions of meaning, experience, and creativity, while keeping the mathematical core of Parts I and II intact.

The framework presented here is intentionally open-ended. It provides a scaffolding in which multiple detailed modeling choices can be tested without discarding the core tri-directional, coherence-based picture of reality that underlies the U.R.H.U.E.0hm series.

Acknowledgments.